



# Evolution of nitric oxide regulation of gut function

Junko Yaguchi<sup>a</sup> and Shunsuke Yaguchi<sup>a,1</sup>

<sup>a</sup>Shimoda Marine Research Center, University of Tsukuba, 5-10-1 Shimoda, Shizuoka 415-0025, Japan

Edited by Marianne E. Bronner, California Institute of Technology, Pasadena, CA, and approved February 5, 2019 (received for review October 2, 2018)

**Although morphologies are diverse, the common pattern in bilaterians is for passage of food in the gut to be controlled by nerves and endodermally derived neuron-like cells. In vertebrates, nitric oxide (NO) derived from enteric nerves controls relaxation of the pyloric sphincter. Here, we show that in the larvae of sea urchins, there are endoderm-derived neuronal nitric oxide synthase (nNOS)-positive cells expressing pan-neural marker, Synaptotagmin-B (SynB), in sphincters and that NO regulates the relaxation of the pyloric sphincter. Our results indicate that NO-dependent pylorus regulation is a shared feature within the deuterostomes, and we speculate that it was a characteristic of stem deuterostomes.**

pylorus | gut | nitric oxide | nitric oxide synthase | sea urchin

To obtain nutrients, bilaterians consume and move food through the digestive tract where it is digested and absorbed. The movement of food appears to be regulated by the nervous and enteroendocrine systems. Gut-associated neurons and enteroendocrine cells are common throughout the metazoa. For example, in protostomes, the enteric placode-derived stomatogastric ganglia and axons of the central nervous system directly innervate the gut (1, 2). In vertebrates, neural crest cell-derived enteric neurons (ENs) and the enteroendocrine cells, which are derived from the endoderm, have important roles in the regulation of gut activity (3). Although the presence of regulatory systems is a common feature, the embryonic origins or the details of their function are not well described in many phyla. As a consequence, we know relatively little about comparative aspects of enteric neurons, enteroendocrine cells, and the evolutionary history of systems for regulating gut motility in metazoans.

Sphincters compartmentalize the digestive tract and control the directional movement of food from mouth to anus. In mammals, NO regulates the pyloric sphincter (4, 5). Enteric neurons express neuronal nitric oxide synthase (nNOS), and nNOS deficiency results in the dysfunction of pyloric sphincter and delayed gastric emptying. Because NO regulates smooth and striated muscles (5, 6) in diverse organisms, it is a suitable candidate for comparative studies of gut function and evolution of the regulatory system of sphincters.

Larvae of sea urchin, which are nonvertebrate deuterostomes, have a tripartite gut similar to that of vertebrates (Fig. 1 *A* and *D*), including an esophagus, stomach, and intestine. The gut compartments are separated by the cardiac and pyloric sphincters (7, 8). The patterns of gene expression and regulatory states throughout the digestive tract are remarkably similar to that of vertebrates (9). The gene expression profile along the gut is also similar to that of tunicates and amphioxus, both nonvertebrate deuterostomes (10, 11). However, it is unclear if sphincters are present in either of these groups. While, the behavior of ingested microbeads indicates a regulated barrier lies between the stomach and the intestine (12). As sea urchins have a distinct pyloric sphincter, they are tractable models for investigating gut formation and function. A number of studies have revealed that sea urchin larvae have a well-developed ectoderm-derived nervous system (13) and Wei et al (14) have reported that the sea urchin foregut produces neurons that associate with the musculature of the esophagus. The means by which ingested food is systematically moved through the digestive tract of sea urchin larvae is not known. In this study, we report that the neuron-like cells

associated with the pylorus of larvae of sea urchins, *Hemicentrotus pulcherrimus*, and *Temnopleurus reevesii* are endodermally derived, and we reveal a role for NO in regulating the pyloric sphincter. These data suggest a hypothesis for the evolutionary history of regulatory system in deuterostomes.

## Results

Initially, we examined the presence of neurons or neuron-like cells in the larval gastrointestinal tract of the sea urchin *H. pulcherrimus* (Infraorder Echinidea) using immunohistochemistry targeting a pan-neural Synaptotagmin B (SynB) with the monoclonal antibody 1E11 (15, 16) and muscle-specific Troponin-I (7) and found two sets of EN-like cells on either side of the pyloric sphincter (Fig. 1 *B–D*): stomach ventral side (sEN hereafter; Fig. 1*B*, arrow) and intestine dorsal side (iEN hereafter; Fig. 1*B*, arrowheads). The average number of sENs and iENs is one and two, respectively (SI Appendix, Fig. S1*A*), and the axon-like processes, which surround the sphincter at 5–7 d postfertilization (dpf), were only observed in the sEN (Fig. 1 *B* and *C* and SI Appendix, Fig. S1 *A* and *B*). The position of those neuron-like cells is adjacent to the Troponin-I-positive pyloric sphincter (Fig. 1 *C* and *D*). These EN patterns are the same in larvae of *T. reevesii* (Infraorder Temnopleuridea) (SI Appendix, Fig. S1*C*), suggesting that ENs are commonly present at the pylorus in the wide range of sea urchin groups because the infraorder *Temnopleuridea* diverged 130 Mya from the infraorder *Echinidea* (17), in which most experimental model sea urchins such as *H. pulcherrimus* belong. The proneural marker *zfhx1* (*zfhx1b*) is expressed in neural progenitors of sea urchins (18), and it is an essential neuronal transcription factor for enteric nervous system formation in mammals (19). With other proneural markers such as *soxC* (20) and *delta* (18), *zfhx1* is expressed in cells in the position of sEN and iEN (SI Appendix, Fig. S1 *D–F*). Because it has been clearly described that these proneural genes are involved in neural specification/differentiation

## Significance

**In vertebrate digestive tracts, pyloric sphincters play an important role in controlling the passage of food from stomach to intestine. A major regulator of sphincter relaxation is nitric oxide (NO). However, it is unknown when and how this important means of control was acquired, in part because we lack information on how nonvertebrate deuterostome sphincters are regulated. Here, we show that a NO-dependent regulatory system is present in the pyloric sphincters of sea urchin larvae. Our data suggest that NO-dependent regulation of the pyloric sphincter was present in deuterostome stem groups, and the common deuterostome ancestor had endodermally derived cells that regulated gut function.**

Author contributions: J.Y. and S.Y. designed research, performed research, analyzed data, and wrote the paper.

The authors declare no conflict of interest.

This article is a PNAS Direct Submission.

Published under the PNAS license.

<sup>1</sup>To whom correspondence should be addressed. Email: yag@shimoda.tsukuba.ac.jp.

This article contains supporting information online at [www.pnas.org/lookup/suppl/doi:10.1073/pnas.1816973116/-DCSupplemental](http://www.pnas.org/lookup/suppl/doi:10.1073/pnas.1816973116/-DCSupplemental).

Published online March 4, 2019.

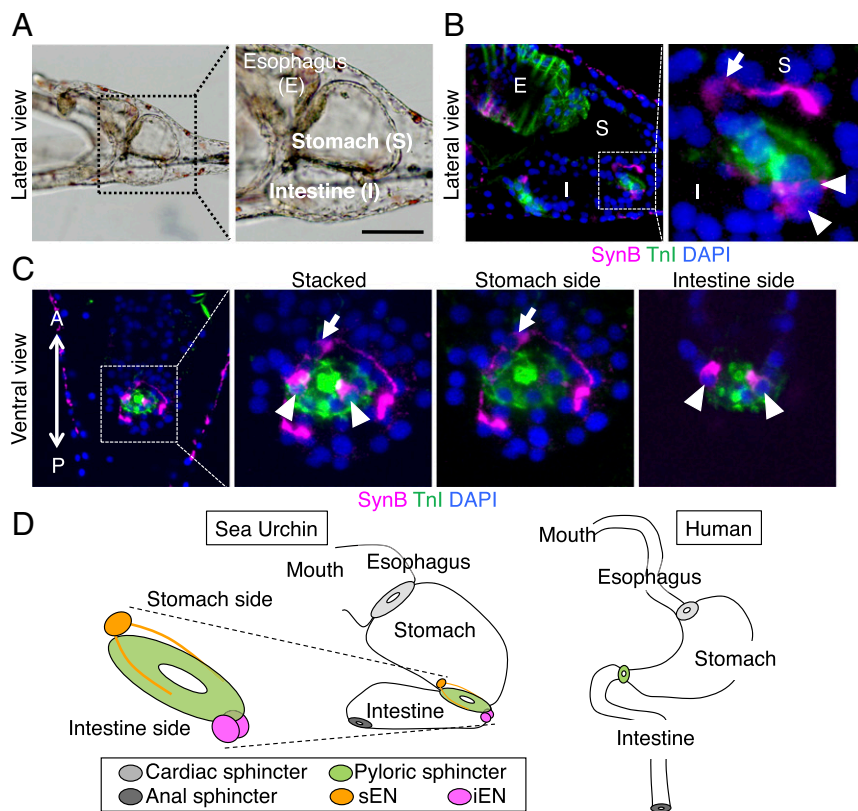


**Fig. 1.** Gastrointestinal enteric neurons are present at the pylorus in sea urchin larvae. (A) Four-day larva has morphologically developed esophagus (O), stomach (S), and intestine (I). (B and C) Neuron-specific SynB (magenta) and muscle-specific Troponin-I (Tnl, green) immunoreactivity in 4-d larva. Tnl indicates the position of the pyloric sphincter. SynB-positive cells are considered enteric neurons. (B) Several optical sections were stacked to visualize the entire pylorus region: lateral view. (C) Optical sections of the entire pylorus, only the stomach side, and only the intestine side were stacked, respectively. Double-headed arrow indicates the anterior (A) and posterior (P) directions: ventral view. (D) Simplified schematic image of the digestive tract of sea urchin and human with highlighted pylorus. Green, yellow, magenta, light gray, and dark gray indicate the pyloric sphincter, sEN, iEN, the cardiac sphincter, and the anal sphincter, respectively. (Scale bar: 50  $\mu$ m.) The arrow shows the stomach-side enteric neuron-like (sEN), and the arrowheads show the intestine-side enteric neuron-like (iEN). Blue, DAPI.

in sea urchins, the expression data suggests that a gene regulatory network involving *Zfhx1*, *SoxC*, and *Delta* functions to produce neuron-like cells within the pylorus. Additionally, TGF- $\beta$  ligands (21) also appear to be involved in the EN formation (details in *SI Appendix*, Fig. S2 A–C).

To investigate the EN cell lineage, we injected mRNA encoding 5 Myc tags as a lineage tracer into one blastomere at the eight-cell stage (Fig. 2A) and detected the protein with SynB in 4 dpf larvae ( $n = 80$ ). As reported in *H. pulcherrimus* (22), the dorsoventral blastomere lineage has principally two patterns: The first cleavage plane is either coincident with or perpendicular to (pattern 1), or  $\sim 45^\circ$  rotated from (pattern 2), the dorsal-ventral axis (Fig. 2A). Since the third cleavage plane segregates blastomeres into ectoderm (Fig. 2A, light blue) and endomesoderm (with a small amount of ectoderm) quartets, the Myc-positive blastomere-derived region was divided into four patterns (Fig. 2A): ectoderm (light blue), ventral endomesoderm (yellow), dorsal endomesoderm (red), and ventral/dorsal endomesoderm (diamond). Immunohistochemistry detecting SynB and Myc at the pylorus revealed that all Myc-positive sEN (in 8 larvae) and iEN (in 24 larvae) were derived from vegetal blastomeres (Fig. 2B and C). This pattern is consistent with sEN and iEN being derived from an endomesoderm lineage, although the vegetal blastomeres may include a small amount of ectoderm. In fact, in larvae, in which vegetal blastomeres produce only endomesoderm due to the anterior shift of the ectoderm-endoderm boundary with the activity of the injected constitutively activated  $\beta$ -catenin (23) (*SI Appendix*, Fig. S3A), sEN included Myc (*SI Appendix*, Fig. S3B, arrow and arrowhead). In addition, in *wnt8-cis* regulatory element-Venus construct injected larvae, in which Venus mainly expresses at Veg2 endomesoderm lineage from very early stages (24), sEN included Venus (Fig. 2D, arrow and arrowhead). These data strongly indicate that the SynB cell was derived from the vegetal endomesoderm lineage.

To further examine the EN cell lineage, we eliminated secondary mesenchyme cells, which are specified through Notch signaling (25–27). To inhibit  $\gamma$ -secretase-dependent Notch signal, we applied a  $\gamma$ -secretase inhibitor, 3,5-Difluorophenylacetyl-L-alanyl-L-S-phenylglycine T-butyl ester (DAPT) and confirmed the disappearance of secondary mesenchyme cell derivatives, such as pigment cells and esophageal muscles (*SI Appendix*, Fig. S3C). In DAPT-treated larvae, we found that ENs did not disappear; rather, their number dramatically increased, because DAPT interferes with Delta-Notch lateral inhibition (28) (Fig. 2E). Since sea urchins have two mesodermal lineages, primary and secondary mesenchyme cells, and the former becomes only spicules (29), we conclude that the pyloric ENs are derived from the endodermal lineage in sea urchins. In fact, while knocking down the function of endoderm-specific *Xlox/Pdx1*, a transcription factor essential for overall pylorus formation (30), we revealed that the morphants lost sEN and iEN (Fig. 2F). Overall, we concluded that pyloric neuron-like cells in sea urchins are derived from endoderm.

To test whether these SynB-positive cells truly function as ENs, we focused on the NO pathway, because it plays a major role in regulation of the vertebrate pylorus (31). Without food, the pylorus is usually closed, but an NO donor, *S*-nitroso-*N*-acetyl-D,L-penicillamine (SNAP), caused the pyloric sphincter to relax and open (Fig. 3A and B). This result suggests that the sea urchin pylorus is regulated with NO, and, in fact, *neuronal Nitric Oxide Synthase* (*nNOS/NOS1*) was expressed in the stomach ventral side cell adjacent to the pyloric sphincter, corresponding to the sEN position until at least day 14 (Fig. 3C and *SI Appendix*, Fig. S4A). Double staining with SynB and *nNOS* (Fig. 3D, arrows) and their consistent responses to DAPT treatment (Fig. 3C) confirmed that *nNOS* is expressed in sEN. To examine the function of *nNOS* in the opening regulation of the pylorus, we knocked down *nNOS* by interfering with its translation using a morpholino antisense oligonucleotide (MO) and observed the

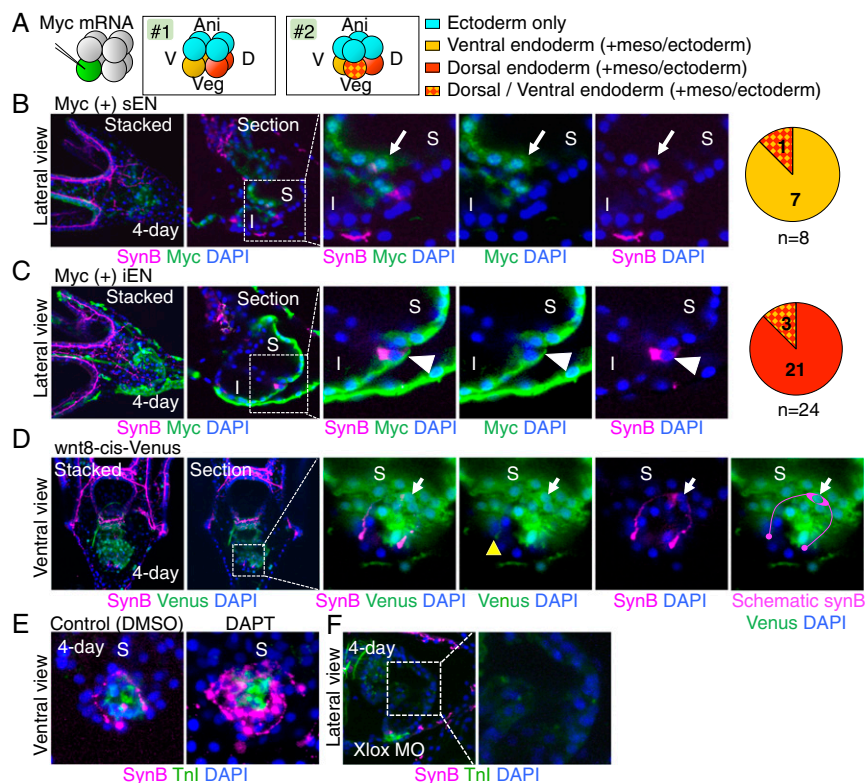


**Fig. 2.** sEN and iEN are derived from the endodermal lineage. (A) Schematic images of Myc-mRNA injection into one blastomere at the eight-cell stage and representative cleavage and lineage patterns in *H. pulcherrimus*. Based on two cleavage patterns along the dorsal-ventral (D-V) axis, the Myc protein is distributed into four categories. Meso/ectoderm indicates mesoderm and ectoderm. (B) Myc signal (green) derived from the vegetal ventral blastomere was detected in sEN (magenta, arrow). (C) Myc signal (green) derived from the vegetal dorsal blastomere was detected in iEN (magenta, arrowhead). Pie charts in B and C, the colors of which refer to the descriptions in A, indicate the number of larvae in which Myc was present in sEN (B) and iEN (C): four-day larva, lateral view. (D) wnt8-cis regulatory element drove Venus signal mainly in endomesoderm lineage, and sEN (arrow) including the axon-like structure (yellow arrowhead) contains Venus. (E) The number of sEN and iEN (magenta) is increased in DAPT-treated larvae. (F) sEN and iEN were not differentiated in Xlox morphants, whereas they were in controls (randomized morpholino injected, Fig. 4B). Ani, animal pole; I, intestine; S, stomach; Veg, vegetal pole. Green in E, pyloric sphincter (Troponin-I). Blue, DAPI.

larval growth rate with feeding. The morphology including the pyloric sphincter and ENs in 4-d nNOS morphants was almost normal (Fig. 4A and B), but the size of the gastrointestinal tract was significantly smaller and this might affect its normal function of food digestion or nutrient intake although the ingested algae could pass through it at this stage (Fig. 4C and *SI Appendix, Fig. S4B*). In fact, intriguingly, unlike the 2-wk control larvae [six-arm rate, 36/38 (94.7%)], morphants of the same age grew into 4-arm larvae but not further [six-arm rate; 0/40 (0%)], similar to unfed larvae (Fig. 4D), suggesting that they fail in normal digestion/nutrition intake essential for larval growth. Gastrointestinal size in the morphants was much smaller than that in controls (*SI Appendix, Fig. S4B*), as observed in visceral muscle-deficient larvae (7), and food rarely entered the intestine at this stage. Since the algae could pass through the gastrointestinal tract in 4 d (Fig. 4C) and food entered the stomach even at 14 d (Fig. 4C and D), presumably the pylorus in the morphants malfunctioned gradually. A lack of nNOS activity in the human pylorus causes hypertrophic pyloric stenosis gradually a few weeks after birth. In affected individuals, ingested milk can normally pass through the gastrointestinal tract immediately after birth (31). As well, dysfunction of pyloric sphincter opening is observed in nNOS<sup>-/-</sup> mice (4), indicating nNOS regulation of gut function is necessary in sea urchins and vertebrates.

## Discussion

Our data indicated that sea urchins have endoderm-derived, nNOS-positive, neuron-like cells at the pylorus, and NO regulates the pyloric sphincter. The correlation of nNOS/NO function involved in pylorus regulation between sea urchins and vertebrates is intriguing. In protostomes, digestive tracts are also partitioned with sphincters and there are enteric neurons (32–34). However, we know of no reports of nNOS/NO regulation of gut function in most protostomes. This suggests that nNOS/NO involvement in regulation of the pyloric sphincter was acquired independently within the deuterostome clade. Although cnidarians

typically lack a pyloric sphincter, NO-associated muscle regulation has been reported throughout the bilaterians and cnidarians (35–38), suggesting that NO-regulated muscle system might have been acquired by stem eumetazoan (39). We cannot completely rule out the possibility that NO-responsive muscles are recruited independently in Ambulacraria and vertebrates, but we favor the former idea because the compartmentalization of the gut or acquisition of a pylorus occurred earlier than the branching point of Ambulacraria and chordates in deuterostome evolution (9).

In this study, we show not only that the sea urchin pyloric sphincter muscle is regulated with NO, but also that nNOS-dependent muscle regulatory system is present in the pylorus, i.e., sEN (Figs. 3 and 4). In addition, the detailed cell-lineage tracing indicated that sEN is derived directly from the endoderm. Pylorus ENs have also been described in hemichordates (40), suggesting that gastrointestinal ENs are common in Ambulacraria, although their detailed lineage tracing and functional analyses have yet to be reported. Amphioxus and tunicates, chordates without neural crest cells, have also ENs (41, 42) whose cell lineages are unclear, raising a possible evolutionary scenario in which endoderm-derived ENs may be a conserved characteristic of deuterostomes. Although all reported enteric neurons are derived from neural crest cells in mammals and birds (43–45), zebrafish morphants, in which neural crest cell-essential genes such as GDNF or Phox2b were attenuated, had significantly decreased ENs, but the few neurons that remained (46, 47) suggests some vertebrates have nonneural crest cell ENs.

The endodermally derived SynB-positive sEN at the pylorus have features of neurons and enteroendocrine cells. Our results indicate the cells (i) express SynB, which is reported as a pan-neural marker in sea urchin embryos/larvae/juveniles (15); (ii) extend long axon-like processes targeting pyloric sphincter muscles (Fig. 1C); and (iii) express nNOS (Fig. 3D), which is expressed by enteric neurons in vertebrates (4, 48). In addition, (iv) proneural genes, *zfhx1* (18), *soxC* (20), and *delta* (18) are expressed in what appear to be sEN precursors (*SI Appendix, Fig. S1 D–F*). The

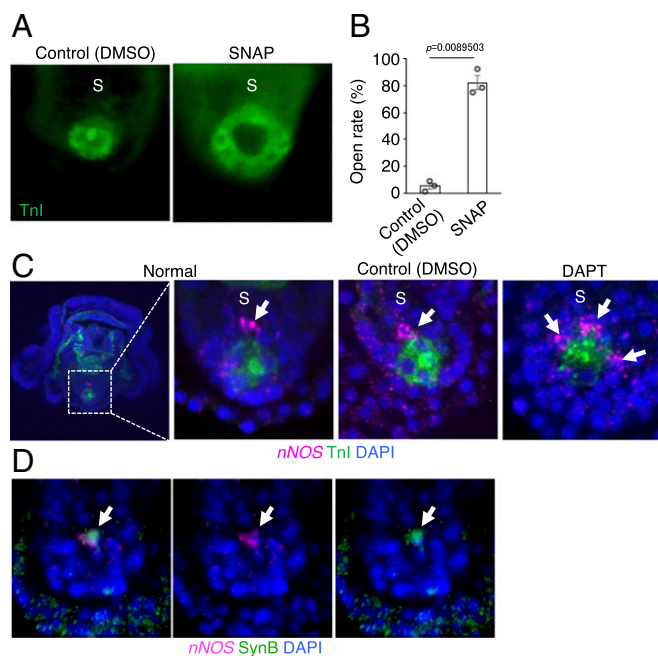


**Fig. 3.** nNOS is expressed in the sEN. (A) One hundred micromolar SNAP (NO donor) relaxes the pyloric sphincter. (B) Graph shows the opening rate of the pylorus at 5 min after the application of DMSO (control) or SNAP.  $n = 3$ . The numbers of larvae with open pylorus in total larvae were 5/123 (4.1%) in the control and 96/116 (82.8%) in SNAP-treated larvae. (C) nNOS is expressed in the cell (magenta, arrow) located in the ventral stomach cell adjacent to the pyloric sphincter (TnI, green) of normal and control (DMSO) treated larvae, and the number of nNOS-positive cells (arrows) is increased in DAPT-treated larvae, implying that nNOS is expressed in sEN. Blue, DAPI. (D) nNOS-mRNA (magenta) is expressed in SynB (green) protein-positive sEN (arrow). Data in B are means  $\pm$  SEM. Exact  $P$  value was calculated by a two-tailed  $t$  test. S, stomach.

neuron-like cells are adjacent to TnI-positive muscle (Fig. 1C), suggesting NO from the nNOS-positive EN directly regulates the pyloric sphincter in the sea urchin larvae. This is similar to the relationship of enteric neurons and the pyloric sphincter in vertebrates (4). However, endoderm-derived cells, which contain neurotransmitters and hormones, are categorized as enteroendocrine cells in vertebrate digestive tracts (3, 49). Some enteroendocrine cells have axon-like processes, which are shorter than neuronal axons, and target the gut lumen and enteric neurons on the basal side of the gut wall (49, 50). It is also reported that hormones released from enteroendocrine cells regulate the contraction and relaxation of the pyloric sphincter (51). Because sEN in sea urchin larvae shares some of these morphological and functional characteristics, we cannot conclude that SynB-positive cells are neurons or enteroendocrine cells. It has been suggested that peripheral sensory neurons and enteroendocrine cells share common origins (50), which makes the difference indistinct. Although we are unable to fully distinguish the nature of these cells, sea urchin nNOS-positive endoderm-derived cells suggests an evolutionary history in which the common deuterostome ancestor had endodermally derived cells that regulated gut function. Thus, nNOS regulation of pyloric function by endodermally derived neuron-like cells appears to be a shared feature of deuterostomes derived from a common stem deuterostome lineage.

## Materials and Methods

**Animal Collection and Embryo/Larva Culture.** Adults of *H. pulcherrimus* were collected around Shimoda Marine Research Center, University of Tsukuba, and around the Marine and Coastal Research Center, Ochanomizu University under the special harvest permission of prefectures and Japan Fishery cooperatives. Adults of *T. reevesii* were collected around Shimoda Marine

Research Center, University of Tsukuba. They are kept in temperature-controlled aquariums (13 °C and 24 °C for *H. pulcherrimus* and *T. reevesii*, respectively) until use, and the used adults were kept until the next breeding season, or released to the place they were collected. Gametes were collected by the intrablastocoelic injection of 0.5 M KCl, and the embryos/larvae of *H. pulcherrimus* and *T. reevesii* were cultured at 15 °C and 22 °C, respectively, in glass beakers or plastic dishes that contained filtered natural seawater (FSW) with 50  $\mu$ g/mL kanamycin. In some experiments, we fed 10  $\mu$ L of SunCulture algae (*Chaetoceros calcitrans*, Marineteck, approximately 30,000 cells per  $\mu$ L) to the larvae as forage in 3.0 mL of FSW almost every day, when the embryos were replaced in fresh FSW in a new plastic dish.

**DAPT and SNAP Treatments.** DAPT (Sigma-Aldrich) was used as a  $\gamma$ -secretase inhibitor. SNAP (Wako Pure Chemical Co.) was used as a NO donor. DAPT and SNAP were prepared as 20 mM and 100 mM stocks in dimethyl sulphoxide (DMSO) and diluted in FSW to 20  $\mu$ M and 100  $\mu$ M before use, respectively (28, 52). To obtain larvae in which the secondary mesenchyme cells failed to develop completely, we treated them with DAPT from 1 h to 24 h after fertilization (25). SNAP was applied to the larvae 5 min before observation. The same volume of DMSO was applied as controls for both DAPT and SNAP.

**Whole-Mount in Situ Hybridization and Immunohistochemistry.** Whole-mount in situ hybridization was performed as described (53) with some modifications. A cDNA mix from several embryonic stages was used to make RNA probes based on the *H. pulcherrimus* genome and transcriptome (54). The samples were incubated with 0.8–1.2 ng/ $\mu$ L final concentration digoxigenin (Dig)-labeled RNA probes of nNOS [HPU\_17332; nNOS (1154–2098 bp), nNOS-second (2395–3177 bp)], *zfhx1* (HPU\_00645) (18), *soxC* (HPU\_08894), and *delta* (HPU\_05341) (18) at 50 °C for 3–7 d. Dig-labeled probes were detected with anti-Dig POD-conjugated antibody (Roche) and treated with Tyramide Signal Amplification Plus System (TSA; PerkinElmer) for 8 min at room temperature (RT). When observed, the samples were incubated in Mops buffer containing 2.5% 1,4-diazabicyclo-2-2-2-octane (DABCO; Wako Pure Chemical Co.) to prevent photobleaching.

Whole-mount immunohistochemistry was also performed as described (53) with some modifications. The samples were blocked with 1% skim milk in PBST [PBS (Nippon Gene Co.), 0.1% Tween-20] for 1 h at RT and incubated with primary antibodies [dilutions: mouse anti-SynB (15) 1:100, rabbit anti-Troponin-I (TnI) (7) 1:200, rabbit anti-pSmad1/5/8 (no. 9511; Cell Signaling Technology) 1:500, rabbit anti-myc (Cell Signaling Technology) 1:500, and rabbit anti-GFP/Venus (MBL) 1:1,500 overnight at 4 °C].

Double staining with SynB protein and nNOS mRNA was performed as described (55) with some modifications. Samples were fixed at 4 °C for 5 h and were blocked with 1% BSA before being incubated with the primary antibody (1:100 dilution of mouse anti-SynB; ref. 15) at the ambient temperature for 1 h. The primary antibody was detected with 1:2,000 diluted goat anti-mouse IgG HRP-conjugated antibody (BioLegend) and TSA treatment. After SynB detection by this TSA-based immunohistochemistry, whole-mount in situ hybridization was performed to detect nNOS as described above.

**Microinjection of MO, mRNAs, and DNA Construct.** For microinjection, we used injection buffer (24% glycerol, 20 mM Hepes pH 8.0, and 120 mM KCl). The morpholino (Gene Tools) sequences and the in-needle concentration with injection buffer were as follows:

nNOS MO1 (1.0–1.5 mM): 5'-AATCGCTCAGAGTTCGGAAGGCAT-3',

nNOS MO2 (0.2–0.3 mM): 5'-GTCGTTCTCCATCGTCAGGCTTTA-3',

Nodal-MO (0.2 mM): 5'-AGATCCGATGAACGATGCATGGTTA-3' (previously characterized in ref. 56),

BMP2/4-MO (0.4 mM): 5'-GACCCCAATGTGAGGTGGTAACCAT-3' (previously characterized in ref. 56), and

Xlox-MO (1.0 mM): 5'-ACGCGGGATTGTTCCCTTCCATGTC-3' (22-base sequence overlapping with the previously characterized Xlox-MO in *Strongylocentrotus purpuratus*) (previously characterized in ref. 57).

Two nonoverlapping translation-blocking morpholinos for nNOS were used to confirm the specificity of their function (SI Appendix, Fig. S4C). For negative control experiments, we injected Random MO (1.0–1.5 mM; Gene Tools) or only injection buffer.

mRNAs were synthesized from linearized plasmids using the mMessage mMachin kit (Thermo Fisher Scientific) and injected at the following

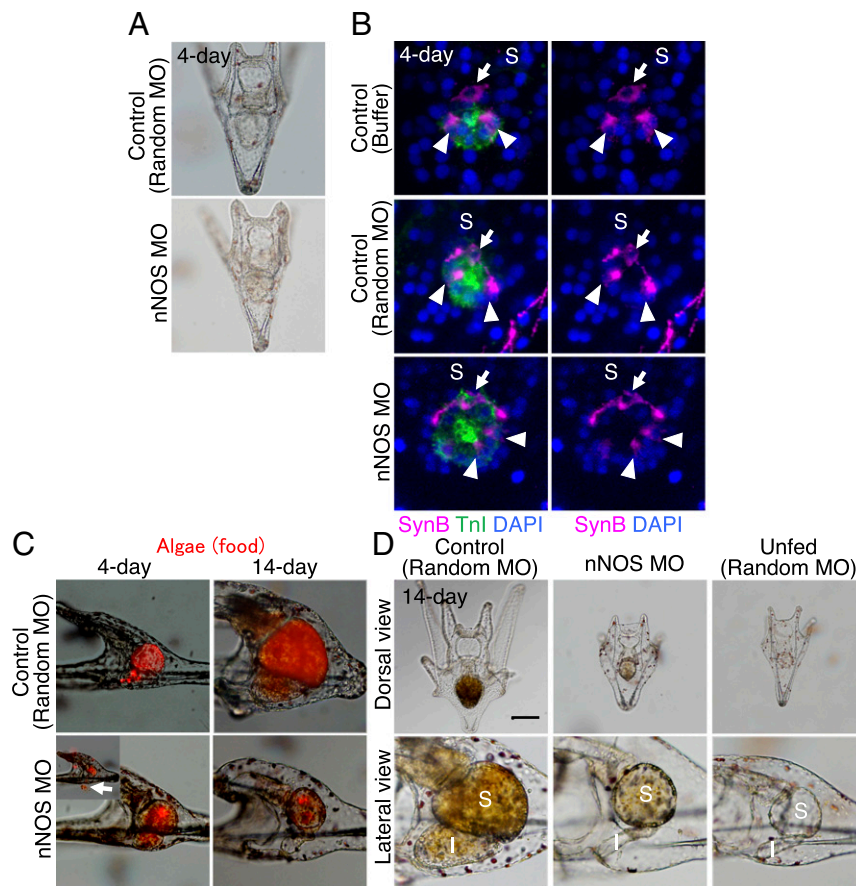


**Fig. 4.** nNOS functions in digestion/nutrition intake. (A) nNOS morphants develop into a four-arm pluteus stage similar to that of controls, except for the stomach and intestine sizes. (B) sEN (magenta, arrow), iEN (magenta, arrowheads) and pyloric sphincter (green) are differentiated normally in nNOS morphants compared with controls in 4-d larvae. Blue, DAPI. (C) Four-day nNOS morphants can ingest algae (*C. calcitrans*), similar to controls [containing algae rate in the stomach, controls: 76/76 (100%), morphants: 82/86 (95.3%)], and defecate as controls (arrow in inset) [containing algae rate in the intestine, controls: 53/76 (69.7%), morphants: 46/82 (56.1%)]. However, 14-d morphants contain algae only in the stomach [control: 7/7 (100%), morphants: 9/10 (90%)] but rarely in the intestine [control: 7/7 (100%), morphants: 1/10 (10%)]. (D) nNOS morphants cannot grow up to reach the six-arm pluteus stage as unfed larvae. (Scale bar: 100  $\mu\text{m}$ .) I, intestine; S, stomach.

concentrations in injection buffer in needles: myc-mRNA (0.1  $\mu\text{g}/\mu\text{L}$ ), act- $\beta$ -catenin (0.4  $\mu\text{g}/\mu\text{L}$ ), BMP2/4-mRNA (1.8  $\mu\text{g}/\mu\text{L}$ ).

wnt8-cis-regulatory element (2,000-bp upstream from start codon) was isolated from *H. pulcherrimus* genome DNA (54) by KOD-FX (TOYOBO)-based PCR using the following primers:

wnt8-cis-F1, 5'-ATTGCATGAAAACATTGGTTGATAAGATCA-3',  
wnt8-cis-R1, 5'-GATGAACACTCCAAAATAAGAAACAAAAA-3',  
wnt8-cis-F2-IF, 5'-TCAAGGCCTCTCGAGCATTGGTTGATAAGA-3', and  
wnt8-cis-R2-IF, 5'-GCCCTTGCTCACCATGATGAACACTCCAAA-3'.

The second two primers were used for PCR to amplify fragment to insert it into pCS-vector with Venus DNA using In-Fusion (Takara). The DNA fragments containing the upstream sequence and Venus were amplified by KOD-FX (TOYOBO) and purified by NucleoSpin Gel and PCR Clean-up (Takara). The solution (0.6 ng/ $\mu\text{L}$  DNA fragment, 12.5 ng/ $\mu\text{L}$  genomic DNA digested by EcoRV, 0.04 M Hepes pH 8.0, and 0.12 M KCl) were injected and confirmed that it sufficiently drives Venus signal mainly at endomesoderm lineage as reported (24).

Microinjections into fertilized eggs were performed as described (56). For microinjections into one blastomere at the eight-cell stage, the attached embryos to the bottom of a plastic dish coated with 1% protamine sulfate from unfertilized eggs were washed with  $\text{Ca}^{2+}$  free artificial sea water (CFASW) three times to replace FSW with CFASW at the eight-cell stage. A few minutes after the final wash with CFASW, we injected the solutions into one of the eight blastomeres within 15 min. After microinjection, the

embryos were washed with FSW three times and stored with 50  $\mu\text{g}/\text{mL}$  kanamycin until the desired stages.

**Detection of Alkaline Phosphatase.** To observe the stomach and intestine under clearer conditions, we detected alkaline phosphatase (AP) activity in the digestive tract. Larvae were fixed with cold 100% ethanol ( $-20^\circ\text{C}$ ) for 5 min and washed three times with PBST. The samples were washed three times with AP buffer (100 mM Tris pH 9.5, 50 mM  $\text{MgCl}_2$ , 100 mM NaCl, 1.0 mM levamisole, 0.1% Tween-20), and the AP signal was detected with NBT/BCIP (Promega).

**Microscopy and Image Analysis.** The specimens were observed using a fluorescence microscope (IX70; Olympus) and a confocal laser scanning microscope (FV10i; Olympus). All transmission images were taken with the IX70, and the sizes of the stomach and intestine were analyzed using ImageJ. The number of *zfhx1*-positive cells was counted under the IX70, and the number of sEN and iEN was counted by analysis of the optical sections scanned with the FV10i. Images and drawings for the figures were made using Adobe Photoshop and Microsoft PowerPoint.

**Statistical Analysis.** No statistical methods were used to predetermine the sample sizes. All *n* numbers are described in the figure legends. To compare the two groups in Fig. 3B, we used Welch's *t* test (two-tailed) with a significance level of 0.05 and with a *t* value = 13.094, degrees of freedom (d.f.) = 2.7136, and *P* = 0.0016. To compare more than two groups, we used one-way ANOVA followed by Tukey's post hoc test with a significance level of 0.05, and the following *F* values (*F*) and d.f. For *SI Appendix, Fig. S2*: sEN, *F* = 11.7054, d.f. = 3; iEN, *F* = 79.7143, d.f. = 3. For *SI Appendix, Fig. S4*: stomach, *F* = 240.4943, d.f. = 4; intestine, *F* = 43.7594, d.f. = 4.

**Data Availability.** Source data for all figures and *SI Appendix* are provided with the paper. Sequence data can be found in the genome database of *H. pulcherrimus*, HpBase ([cell-innovation.nig.ac.jp/HpBase/](http://cell-innovation.nig.ac.jp/HpBase/)) (54).

**ACKNOWLEDGMENTS.** We thank R. D. Burke for reading manuscript; Y. Nakajima, R. D. Burke, and H. Tanaka for the essential reagents; and

- Hartenstein V (1997) Development of the insect stomatogastric nervous system. *Trends Neurosci* 20:421–427.
- Copenhaver PF (2007) How to innervate a simple gut: Familiar themes and unique aspects in the formation of the insect enteric nervous system. *Dev Dyn* 236:1841–1864.
- Latorre R, Sternini C, De Giorgio R, Greenwood-Van Meerveld B (2016) Enteroendocrine cells: A review of their role in brain-gut communication. *Neurogastroenterol Motil* 28: 620–630.
- Mashimo H, Kjellin A, Goyal RK (2000) Gastric stasis in neuronal nitric oxide synthase-deficient knockout mice. *Gastroenterology* 119:766–773.
- Sobchak C, Fajardo AF, Shifrin Y, Pan J, Belik J (2016) Gastric and pyloric sphincter muscle function and the developmental-dependent regulation of gastric content emptying in the rat. *Am J Physiol Gastrointest Liver Physiol* 310:G1169–G1175.
- Evangelista AM, et al. (2010) Direct regulation of striated muscle myosins by nitric oxide and endogenous nitrosolithols. *PLoS One* 5:e11209.
- Yaguchi S, Yaguchi J, Tanaka H (2017) Troponin-I is present as an essential component of muscles in echinoderm larvae. *Sci Rep* 7:43563.
- Burke RD (1981) Structure of the digestive tract of the pluteus larva of *Dendrostar excentricus* (Echinodermata: Echinoidea). *Zoomorphology* 98:209–225.
- Annunziata R, et al. (2014) Pattern and process during sea urchin gut morphogenesis: The regulatory landscape. *Genesis* 52:251–268.
- Nakayama S, Ogasawara M (2017) Compartmentalized expression patterns of pancreatic- and gastric-related genes in the alimentary canal of the ascidian *Ciona intestinalis*: Evolutionary insights into the functional regionality of the gastrointestinal tract in Olfactores. *Cell Tissue Res* 370:113–128.
- Holland PWH (2015) Did homeobox gene duplications contribute to the Cambrian explosion? *Zoological Lett* 1:1–8.
- Messinetti S, Mercurio S, Parolini M, Sugni M, Pennati R (2018) Effects of polystyrene microplastics on early stages of two marine invertebrates with different feeding strategies. *Environ Pollut* 237:1080–1087.
- Angerer LM, Yaguchi S, Angerer RC, Burke RD (2011) The evolution of nervous system patterning: Insights from sea urchin development. *Development* 138:3613–3623.
- Wei Z, Angerer RC, Angerer LM (2011) Direct development of neurons within foregut endoderm of sea urchin embryos. *Proc Natl Acad Sci USA* 108:9143–9147.
- Nakajima Y, Kaneko H, Murray G, Burke RD (2004) Divergent patterns of neural development in larval echinoids and asteroids. *Evol Dev* 6:95–104.
- Burke RD, et al. (2006) Neuron-specific expression of a synaptotagmin gene in the sea urchin *Strongylocentrotus purpuratus*. *J Comp Neurol* 496:244–251.
- Kroh A, Smith AB (2010) The phylogeny and classification of post-Palaeozoic echinoids. *J Syst Palaeontology* 8:147–212.
- Yaguchi J, Angerer LM, Inaba K, Yaguchi S (2012) Zinc finger homeobox is required for the differentiation of serotonergic neurons in the sea urchin embryo. *Dev Biol* 363:74–83.
- Stanchina L, Van de Putte T, Goossens M, Huylebroeck D, Bondurand N (2010) Genetic interaction between Sox10 and Zfxh1b during enteric nervous system development. *Dev Biol* 341:416–428.
- Wei Z, Angerer LM, Angerer RC (2016) Neurogenic gene regulatory pathways in the sea urchin embryo. *Development* 143:298–305.
- Duboc V, Röttinger E, Besnardeau L, Lepage T (2004) Nodal and BMP2/4 signaling organizes the oral-aboral axis of the sea urchin embryo. *Dev Cell* 6:397–410.
- Kominami T (1988) Determination of dorso-ventral axis in early embryos of the sea urchin, *Hemicentrotus pulcherrimus*. *Dev Biol* 127:187–196.
- Wikramanayake AH, Huang L, Klein WH (1998) beta-Catenin is essential for patterning the maternally specified animal-vegetal axis in the sea urchin embryo. *Proc Natl Acad Sci USA* 95:9343–9348.
- Minokawa T, Wikramanayake AH, Davidson EH (2005) cis-Regulatory inputs of the wnt8 gene in the sea urchin endomesoderm network. *Dev Biol* 288:545–558.
- Ohguro Y, Takata H, Kominami T (2011) Involvement of Delta and Nodal signals in the specification process of five types of secondary mesenchyme cells in embryo of the sea urchin, *Hemicentrotus pulcherrimus*. *Dev Growth Differ* 53:110–123.
- Sweet HC, Gehring M, Ettensohn CA (2002) LvDelta is a mesoderm-inducing signal in the sea urchin embryo and can endow blastomeres with organizer-like properties. *Development* 129:1945–1955.
- Sethi AJ, Wikramanayake RM, Angerer RC, Range RC, Angerer LM (2012) Sequential signaling crosstalk regulates endomesoderm segregation in sea urchin embryos. *Science* 335:590–593.
- Yaguchi S, et al. (2011) Fez function is required to maintain the size of the animal plate in the sea urchin embryo. *Development* 138:4233–4243.
- Davidson EH, Cameron RA, Ransick A (1998) Specification of cell fate in the sea urchin embryo: Summary and some proposed mechanisms. *Development* 125:3269–3290.
- M. Kiyomoto, T. Sato, D. Shibata, M. Ooue, T. Kodaka, J. Takano, M. Yamaguchi, and JF Izu/Shimoda for collecting and keeping the adult sea urchins. This work is supported, in part, by Takeda Science Foundation and Kishimoto Foundation (Senri Life Science Foundation) (S.Y.), and Japan Society for the Promotion of Science (JSPS) Grant-in-Aid for Scientific Research JP16K18592 (to J.Y.). J.Y. is a JSPS Research Fellow with research Grant 17J00034.
- Arnone MI, et al. (2006) Genetic organization and embryonic expression of the ParaHox genes in the sea urchin *S. purpuratus*: Insights into the relationship between clustering and colinearity. *Dev Biol* 300:63–73.
- Vanderwinden J-M, Mailleux P, Schiffmann SN, Vanderhaeghen J-J, De Laet M-H (1992) Nitric oxide synthase activity in infantile hypertrophic pyloric stenosis. *N Engl J Med* 327:511–515.
- Martinez-Pereira MA, et al. (2013) General morphology and innervation of the midgut and hindgut of *Megalobulimus abbreviatus* (Gastropoda, Pulmonata). *Zool Sci* 30:319–330.
- Martinez-Pereira MA, Franceschi RDC, Coelho BP, Zancan DM (2017) The stomatogastric and enteric nervous system of the pulmonate snail *Megalobulimus abbreviatus*: A neurochemical analysis. *Zool Sci* 34:300–311.
- Nomaksteinsky M, et al. (2013) Ancient origin of somatic and visceral neurons. *BMC Biol* 11:53.
- Feelisch M, Martin JF (1995) The early role of nitric oxide in evolution. *Trends Ecol Evol* 10:496–499.
- Palumbo A (2005) Nitric oxide in marine invertebrates: A comparative perspective. *Comp Biochem Physiol A Mol Integr Physiol* 142:241–248.
- Antcil M, Poulain I, Pelletier C (2005) Nitric oxide modulates peristaltic muscle activity associated with fluid circulation in the sea pansy *Renilla koellikeri*. *J Exp Biol* 208: 2005–2017.
- Davies S (2000) Nitric oxide signalling in insects. *Insect Biochem Mol Biol* 30: 1123–1138.
- Inoue J, Satoh N (2018) Deuterostome genomics: Lineage-specific protein expansions that enabled chordate muscle evolution. *Mol Biol Evol* 35:914–924.
- Nakajima Y, Humphreys T, Kaneko H, Tagawa K (2004) Development and neural organization of the tornaria larva of the Hawaiian hemichordate, *Ptychodera flava*. *Zool Sci* 21:69–78.
- Wicht H, Lacalli TC (2005) The nervous system of amphioxus: Structure, development, and evolutionary significance. *Can J Zool* 83:122–150.
- Bone Q (1959) Observations upon the nervous systems of pelagic tunicates by QUENTIN BONE. *Q J Microscop Sci* 100:167–181.
- Pattyn A, Morin X, Cremer H, Goridis C, Brunet JF (1999) The homeobox gene Phox2b is essential for the development of autonomic neural crest derivatives. *Nature* 399: 366–370.
- Green SA, Uy BR, Bronner ME (2017) Ancient evolutionary origin of vertebrate enteric neurons from trunk-derived neural crest. *Nature* 544:88–91.
- Yntema CL, Hammond WS (1954) The origin of intrinsic ganglia of trunk viscera from vagal neural crest in the chick embryo. *J Comp Neurol* 101:515–541.
- Shepherd IT, Beattie CE, Raible DW (2001) Functional analysis of zebrafish GDNF. *Dev Biol* 231:420–435.
- Elworthy S, Pinto JP, Pettifer A, Cancela ML, Kelsh RN (2005) Phox2b function in the enteric nervous system is conserved in zebrafish and is sox10-dependent. *Mech Dev* 122:659–669.
- McCann CJ, et al. (2017) Transplantation of enteric nervous system stem cells rescues nitric oxide synthase deficient mouse colon. *Nat Commun* 8:15937.
- Bohórquez DV, Liddle RA (2011) Axon-like basal processes in enteroendocrine cells: Characteristics and potential targets. *Clin Transl Sci* 4:387–391.
- Hartenstein V, Takashima S, Hartenstein P, Asanad S, Asanad K (2017) bHLH pro-neural genes as cell fate determinants of entero-endocrine cells, an evolutionarily conserved lineage sharing a common root with sensory neurons. *Dev Biol* 431:36–47.
- Fisher RS, Lipshutz W, Cohen S (1973) The hormonal regulation of pyloric sphincter function. *J Clin Invest* 52:1289–1296.
- Bishop CD, Brandhorst BP (2001) The role of NO/cGMP and HSP90 in regulating metamorphosis of the sea urchin *Lytechinus pictus*. *Dev Biol* 235:251.
- Yaguchi J, Takeda N, Inaba K, Yaguchi S (2016) Cooperative wnt-nodal signals regulate the patterning of anterior neuroectoderm. *PLoS Genet* 12:e1006001.
- Kinjo S, Kiyomoto M, Yamamoto T, Ikeo K, Yaguchi S (2018) HpBase: A genome database of a sea urchin, *Hemicentrotus pulcherrimus*. *Dev Growth Differ* 60:174–182.
- Yaguchi S, Katow H (2003) Expression of tryptophan 5-hydroxylase gene during sea urchin neurogenesis and role of serotonergic nervous system in larval behavior. *J Comp Neurol* 466:219–229.
- Yaguchi S, et al. (2010) ankAT-1 is a novel gene mediating the apical tuft formation in the sea urchin embryo. *Dev Biol* 348:67–75.
- Cole AG, Rizzo F, Martinez P, Fernandez-Serra M, Arnone MI (2009) Two ParaHox genes, SpLox and SpCdx, interact to partition the posterior endoderm in the formation of a functional gut. *Development* 136:541–549.